J. Fluid Mech. (1978), *vol.* 89, *part* 2, *pp.* 373–399
Printed in Great Britain

On the tones and pressure oscillations induced by flow over rectangular cavities

By CHRISTOPHER K. W. TAM

Department of Mathematics, Florida State University, Tallahassee,

AND PATRICIA J. W. BLOCK

NASA Langley Research Center, Hampton, Virginia 23665

(Received 21 April 1977 and in revised form 30 January 1978)

Experimental measurements of the frequencies of discrete tones induced by flow over rectangular cavities were carried out over a range of low subsonic Mach numbers to provide a reliable data base for (aircraft wheel well) cavity noise consideration. A mathematical model of the cavity tones and pressure oscillation phenomenon based on the coupling between shear layer instabilities and acoustic feedback is developed to help in understanding the tone generation mechanism. Good agreement is found between discrete tone frequencies predicted by the model and experimental measurements over a wide range of Mach numbers. Evidence of tones generated by the cavity normal mode resonance mechanism at very low subsonic Mach numbers is also presented.

1. Introduction

This paper studies the acoustic oscillations induced by flow over rectangular cavities. The primary motivation is to obtain a clear understanding of the generation mechanism of wheel well noise of an aircraft. Recent flight measurements conducted by Healy (1974), Gibson (1974) and others indicated that wheel well noise is an important source of airframe noise during landing approach. The noise generated by the interaction of flow over the wheel well consists of discrete and broad band components. The present study focuses on the discrete components alone. These components are associated with strong acoustic oscillations inside the wheel well cavity. The total phenomenon is very complicated. As a first step towards understanding the generation mechanisms of the discrete noise component, the wheel well has been modelled as a rectangular cavity and the unperturbed flow outside the cavity regarded as effectively uniform. This study will include acoustic oscillations induced by both subsonic and supersonic flows; however, for practical purposes, primary interest will be concentrated on shallow cavities with length to depth ratio (L/D) in the vicinity of unity and greater and external flow in the low subsonic Mach number range.

The phenomenon of flow-induced noise radiation and acoustic oscillations in a rectangular cavity has been studied by numerous investigators in the past, e.g. Krishnamurty (1955), Roshko (1955), Dunham (1962), Plumblee, Gibson & Lassiter (1962), Rossiter (1964), Spee (1966), East (1966), Covert (1970), Heller, Holmes &

Covert (1971), Bilanin & Covert (1973), Heller & Bliss (1975), Block (1976) and others. However, unlike the present work, most of these researchers confined their interest to flows with moderate subsonic to high supersonic Mach numbers. The experimental work of East is, perhaps, the only exception. Unfortunately, he limited himself to deep cavities with length to depth ratio less than unity and hence his finding is somewhat less relevant to wheel well noise.

Plumblee *et al.* (1962) earlier proposed that the observed discrete tones were the result of cavity resonance. They suggested that the frequencies of the tones were identical to those which corresponded to the maximum acoustic response of the cavity. According to their theory the entire turbulent shear layer which spans the open end of the cavity provides a broad band noise source which drives the cavity oscillations. The response of the rectangular cavity to this broad band excitation is instrumental in selecting certain narrow band frequencies for amplification. However, as pointed out by Rossiter (1964) and Heller *et al.* (1971), this line of reasoning meets obvious difficulties when the boundary-layer flow adjacent to the outside wall is laminar. Experiments revealed that laminar flow produces louder tones even though the broad band excitation as required by the Plumblee *et al.* model is absent. Despite this problem, East (1966) obtained evidence that the depth mode (lowest normal mode) of not too shallow cavities is often excited at very low subsonic Mach numbers. This finding is confirmed experimentally by the present work. A somewhat modified normal mode resonance model similar to the idea of Plumblee *et al.* will be presented later to explain the observed phenomenon.

At slightly higher subsonic Mach numbers ($M > 0{\cdot}15$) to high supersonic Mach numbers, discrete tones exhibit characteristics which cannot be explained by the normal mode resonance concept. For these flow Mach numbers, a sequence of tones is usually observed. These tones are not harmonics of each other although harmonics can be found. If the observed Strouhal numbers (based on the flow velocity and length of the cavity) of these tones are plotted against the flow Mach numbers, the data points lie on well-defined bands as shown in figure 1. Rossiter (1964) seemed to be one of the early investigators who suggested that the observed phenomenon was a result of acoustic feedback. His shadowgraphic observations (Mach numbers ranged from 0·4 to 1·2) indicated that concentrated vortices were shed periodically in the vicinity of the upstream lip of the cavity. These vortices travelled downstream along the shear layer which spanned the open end of the cavity. On the basis of this and other observations, Rossiter proposed the following model which he believed was responsible for generating the cavity tones. Vortices, shed periodically from the upstream lip of the cavity, are convected downstream in the shear layer until they reach the downstream end of the cavity. Upon interacting with the downstream wall of the cavity acoustic pulses are generated. These acoustic disturbances propagate upstream inside the cavity. When reaching the upstream end of the cavity, the acoustic pulses cause the shear layer to separate upstream of the edge resulting in the shedding of new vortices. In this way the vortices and acoustic disturbances form a feedback loop. Using the fact that the timing of the various links of the feedback loop must be synchronized, Rossiter derived the following semi-empirical formula for the tone frequencies:

$$\frac{fL}{U_\infty} = \frac{m-\gamma}{M+1/\kappa},$$

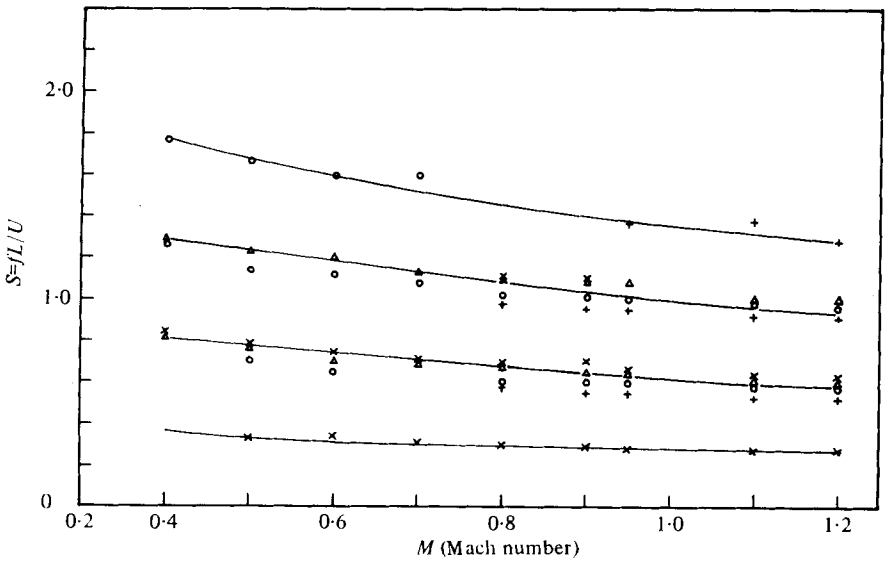

FIGURE 1. Frequency of periodic pressure fluctuations in rectangular cavities (Rossiter 1964). L/D: ×, = 4; △, = 6; ○, = 8; +, = 10.

where f = frequency of tones, L = length of cavity, U_∞ = free-stream velocity, m = integer, M = Mach number, κ = ratio of convection velocity of vortices to free-stream velocity, γ = a factor to account for the lag time between the passage of a vortex and the emission of a sound pulse at the downstream corner of the cavity. The model, however, does not provide numerical values for κ and γ. They are treated as empirical constants to be determined by a best fit to measured data. Rossiter found that by taking $\gamma = 0{\cdot}25$ and $1/\kappa = 1{\cdot}75$, the above equation agreed with his measured data very well as shown in figure 1.

The success of Rossiter's semi-empirical formula in predicting his own data does not necessarily mean that his model is correct. Actually his equation is not always so successful when compared with data obtained by others and especially when the flow Mach number is outside the range covered in figure 1. Figure 2 shows a comparison of this equation using the same value of γ and $1/\kappa$ adopted by Rossiter with data obtained in the present study for Mach numbers less than 0·4. These data will be extensively described in a later section of this paper. In the Rossiter model, a good deal of significance is attached to the highly localized vortices. However, schlieren pictures taken by Krishnamurty (1955) did not indicate the presence of these vortices during cavity oscillations. Heller & Bliss (1975) employed water table visualization techniques to study the phenomenon when the external flow is supersonic. No vortex shedding was found even though the fluid in the cavity and the free shear layer spanning the cavity underwent violent oscillations. This finding is also supported by the schlieren observations of Heller *et al.* (1971) for high subsonic and supersonic flows. The accumulated evidence seems to be at variance with the Rossiter model and indicates that vortex shedding is probably not important over the entire Mach number range as far as cavity oscillations are concerned. In addition, the Rossiter model does not describe how acoustic disturbances are generated at the downstream wall of the cavity and how the feedback acoustic waves excite the shear layer at the upstream

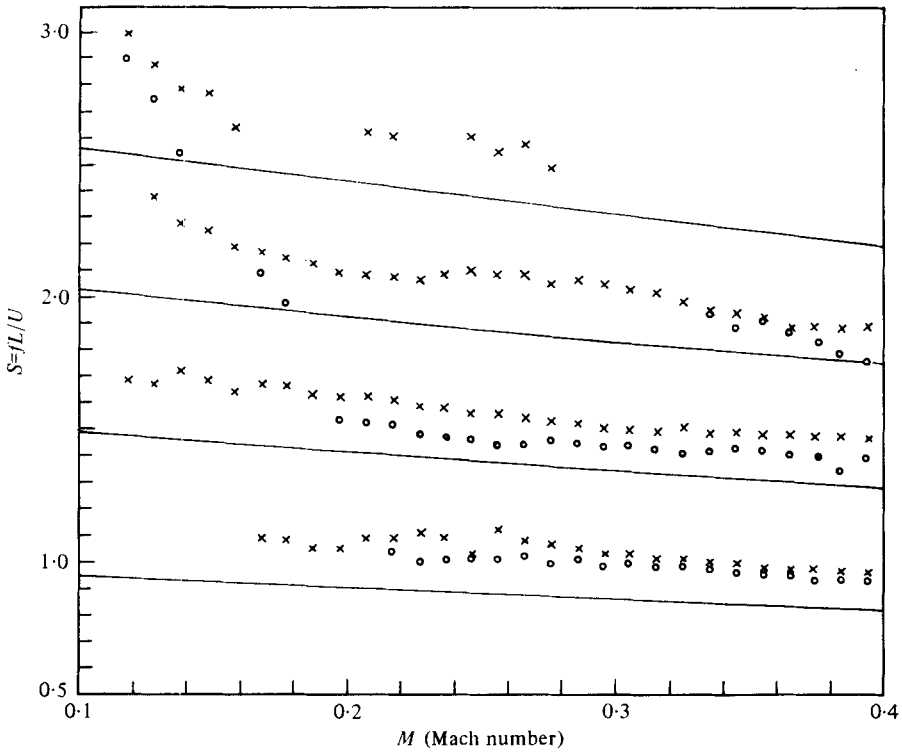

FIGURE 2. Comparison of Rossiter's semi-empirical formula and present data. ——, Rossiter's formula (1964). Data: ×, ○; $L/D = 2{\cdot}36$ (see also figure 16).

lip. Although, for the purpose of predicting the frequencies of discrete tones, the details of these physical processes may not be extremely crucial, knowledge of these processes is of vital importance to noise suppression efforts.

Bilanin & Covert (1973), at the suggestion of one of the present authors, improved on Rossiter's feedback model by relating the driving mechanism of cavity oscillations to the instabilities of the free shear layer. It is well known that free shear layers of the kind that exist at the mouth of the cavity are prone to Kelvin–Helmholtz instabilities. Although it might not have been explicitly stated, the importance of flow instabilities was recognized quite some time ago, e.g. Krishnamurty (1955). The Bilanin & Covert model assumed that the shear layer is being agitated periodically at the upstream lip of the cavity. This excites the flow instability waves of the shear layer which grow as they propagate downstream. The fluctuating motion of the shear layer at the downstream wall of the cavity induces a periodic inflow of external fluid into the cavity and half a period later a discharge of cavity fluid into the external flow. Bilanin & Covert attributed this action of mass inflow and outflow as the source of acoustic radiation. As in the Rossiter model the acoustic disturbances are assumed to propagate upstream inside the cavity without disturbing the shear layer. On reaching the upstream wall the acoustic wave is envisaged to give rise to a localized pressure force which excites the shear layer. Thereby the feedback loop is closed. In developing this model mathematically Bilanin & Covert idealized the shear layer as a thin vortex sheet. For the noise source at the downstream corner of the cavity,

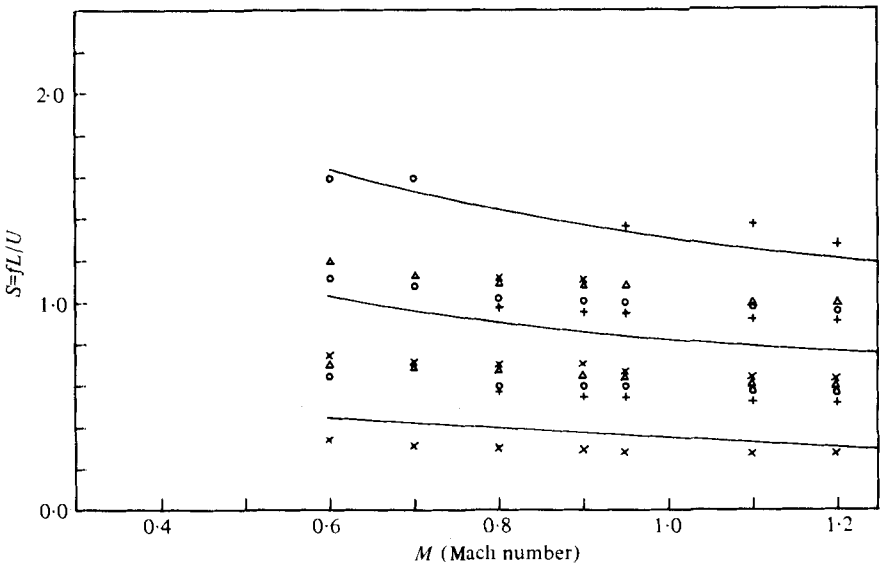

FIGURE 3. Comparison of Rossiter's data and the theory of Bilanin & Covert. ——, Bilanin & Covert (1973); ×, △, ○, +, Rossiter's data (see legend of figure 1).

they used a line source which pulsated periodically. To complete the model, a line pressure force was adopted at the upstream lip of the cavity to simulate the excitation of the shear layer by the acoustic waves. Upon invoking the condition that the phase of the feedback loop must increase by an integral multiple of 2π when traversing it once around, Bilanin & Covert computed the discrete tone frequencies of cavity oscillations. It is to be noted that their predictions are free of any empirical constant. In their paper Bilanin & Covert showed that their predictions agreed reasonably well with measurements for high supersonic Mach number flows. However, for low supersonic and high subsonic Mach numbers, their theoretical results do not seem to compare as favourably with experimental data. Figure 3 shows a comparison between Rossiter's data and the prediction of Bilanin & Covert. It can be seen that the discrepancy between theory and experiment is considerable within the range of Mach numbers shown.

The model of Bilanin & Covert is an improvement over Rossiter's. Yet, like Rossiter, they never treated the question of how the acoustic disturbances interacted and excited the flow instabilities. In addition, they overlooked one fundamental problem in their vortex sheet model. For an infinitesimally thin vortex sheet, it has been shown by Miles (1958) that the flow becomes stable at a sufficiently high Mach number. If the total temperatures of the fluids above and below the vortex sheet are equal, the flow is stable for $M > 2^{1\cdot5}$. When the vortex sheet is stable there is no driving mechanism for cavity oscillations in the Bilanin & Covert model, which contradicts experimental observations. Bilanin & Covert ignored this change in the instability characteristics of a thin shear layer and applied their model to flows with Mach number as high as 3·4. Block (1976) extended the Bilanin & Covert model to include the effect of the length to depth ratio. Although agreement with experimental data was somewhat improved, the model suffers the same inadequacies as the Bilanin & Covert model.

The purpose of this work is to study the phenomenon of acoustic oscillations induced by flow over rectangular cavities both experimentally and theoretically. The experimental part of this paper concentrates on reporting the observed tone frequency characteristics for flow Mach number less than 0·4. Good and reliable data have not been readily available in the literature over this range of low subsonic Mach numbers. Of particular interest is the observation of a transition from the normal mode resonance mechanism to the feedback instability mechanism for discrete tone generation as flow Mach number increases. Details of these will be described in §§4 and 5 below. Further discussion of the normal mode resonance mechanism in relation to the measurements will be given. In §§2 and 3, a mathematical model of acoustic feedback oscillations is developed. This model incorporates the feature of shear layer instabilities of the Bilanin & Covert model. However, unlike the Bilanin & Covert model, the thickness of the shear layer is taken into account. This effect turns out to be important. In addition, the excitation of shear layer instabilities by acoustic disturbances is analysed rigorously. The simplifying assumption of point force excitation used by Bilanin & Covert is removed. Further, the reflexion of acoustic waves by the bottom wall of the rectangular cavities is also taken into consideration. Thus the present model has two additional parameters, namely the ratio of the momentum thickness of the shear layer to the length of the cavity θ/L and the cavity length to depth ratio L/D, which are ignored by most previous models. In §5 the predicted tone frequencies based on this model are compared with measurements over the whole subsonic to low supersonic Mach number range. Quite favourable agreement is found lending support to the contention that the present model indeed accounts for most of the essential features of the acoustic oscillation phenomenon.

2. A mathematical model

The flow field associated with pressure oscillations in a rectangular cavity is highly unsteady and complex. It is not possible at the present time to solve this flow surface interaction problem from first principles. The objective here is to develop a sufficiently simple mathematical model of the acoustic feedback mechanism. A model of this kind is valuable in that it provides an understanding of the basic controlling processes.

In developing the feedback model below it will be assumed that the rectangular cavity is two-dimensional and that the mean flow inside the cavity (see figure 4) can be ignored. Strictly speaking this is not correct as pointed out by Maull & East (1963). In a follow-up work on the unsteady component of cavity oscillations, East (1966), however, found that there was no correlation between the mean flow and the acoustic behaviour of the cavity. His experimental results showed that the tones of the acoustic feedback oscillations were totally unaffected by the three-dimensional mean flow. Based on this conclusion a two-dimensional model is deemed adequate at this time.

Before entering into a detailed discussion of the proposed mathematical model, it is instructive to ask what are the important dimensionless parameters of the problem. As far as is known most previous work on feedback oscillations considered the dependence of the Strouhal numbers of the discrete tones on flow Mach numbers only. Figure 5 shows a collection of data on the Strouhal numbers from various sources plotted as a function of Mach number. It is seen that there is a large scattering of the

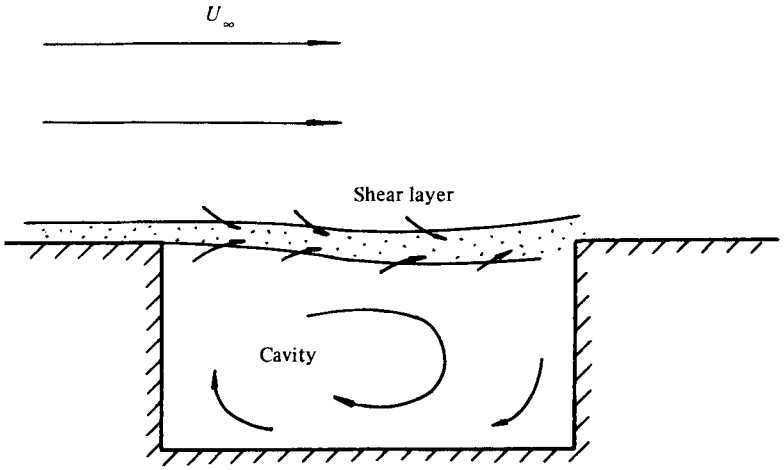

FIGURE 4. Entrainment flow and captive vortex.

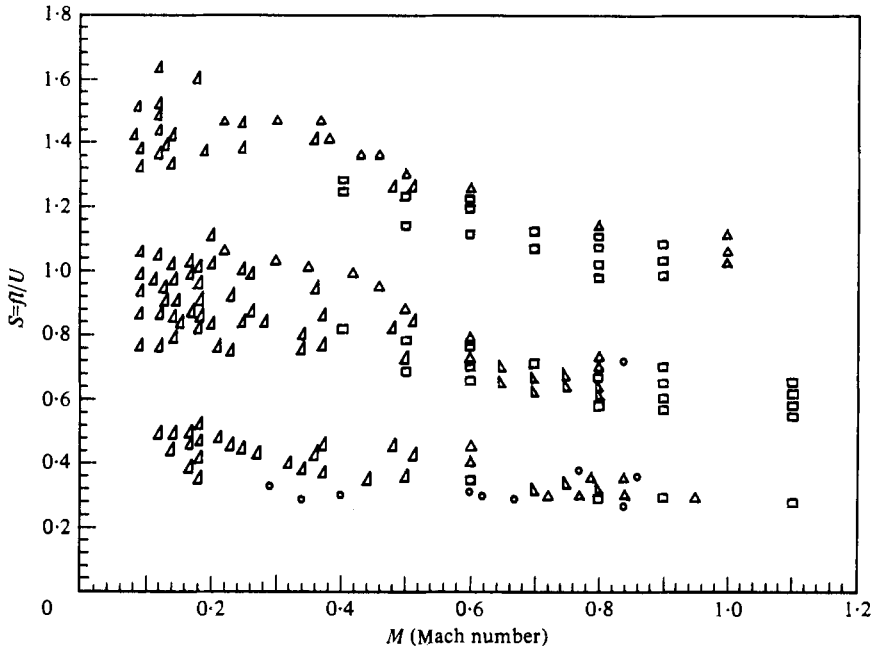

FIGURE 5. Experimental results from several investigations of cavity oscillation frequencies. △, Heller & Bliss (1975); ◺, Krishnamurty (1955); ○, Plumblee *et al.* (1962); □, Rossiter (1964); ◿, Block (1976).

data. This indicates that the flow-induced acoustic oscillation phenomenon is affected not only by the Mach number but by other parameters as well. A parameter of possible importance is the length to depth ratio of the cavity L/D, which arises because of reflexion of sound waves by the bottom wall of the cavity as has been discussed by Block (1976). In the proposed model described below it will be established that the ratio of cavity length to the thickness of the shear layer is also an important parameter in so far as determining the tone Strouhal number is concerned. Unfortunately in

most of the experiments cited in figure 5 the thicknesses of the shear layers were not measured. Lack of this information makes it difficult to correlate these data in a satisfactory manner.

The phenomenon occurring at the cavity trailing edge is also an important consideration. Krishnamurty (1955), in his pioneering work on cavity oscillations, recognized that the interaction between the oscillating shear layer and the trailing edge of the cavity produced intense acoustic disturbances. This idea was adopted by Rossiter (1964) and later by Bilanin & Covert (1973) as an important link in their feedback models. Although experimental evidence leaves no room for doubt concerning the existence of this acoustic source, there is very little agreement as to how the pressure waves are generated. Rossiter did not attempt to describe the process in his vortex/trailing-edge interaction model. Bilanin & Covert assumed the unsteady mass addition and removal at the trailing edge of the cavity as the cause of the acoustic disturbance which essentially suggests a dipole source at the trailing edge. For the purpose of computing the phase of the pressure disturbances which excite the shear layer they only consider the acoustic waves inside the cavity. However, one should consider the disturbances generated outside the cavity as well in the case of subsonic flow. To see this it is only necessary to observe that a mass inflow into the cavity is at the same time a mass outflow from the point of view of the external flow and vice versa. Thus a compression wave produced inside the cavity due to an inflow of outside fluid at the trailing edge of the cavity is accompanied by the generation of a rarefaction wave outside the cavity. According to the Bilanin & Covert model the acoustic waves outside and inside the cavity are therefore exactly opposite in phase as in the case of dipole radiation. Unfortunately, this is at odds with the schlieren observations of Krishnamurty (1955) at subsonic flows. In addition, using the water table visualization technique, Heller & Bliss were able to simulate the sequence of events which took place during a typical oscillation cycle. They found that the compression wave (shock wave) produced at the trailing edge of the cavity extended from inside the cavity all the way to the supersonic outside flow. Before they are modified by the outside mean flow, observations clearly indicate that the pressure disturbances inside and outside the cavity are in phase, contrary to the model of Bilanin & Covert. More recently, Heller & Bliss (1975) attempted to model the process of acoustic wave generation by assuming the back wall of the cavity as behaving like a pseudo-piston. But the effort failed to predict any discrete oscillation frequency.

In this paper, the following acoustic wave generation process is proposed. As evidenced by flow visualization, the shear layer oscillates up and down near the trailing edge of the cavity. During the upward motion of the cycle the fluid of the shear layer shields the trailing edge of the cavity from the external flow as shown in figure 6 (*a*). Under this circumstance the external fluid flows smoothly over the trailing edge and no pressure waves of any significance are generated. When the shear layer is deflecting downward there is an inflow of external fluid into the cavity as shown in figure 6 (*b*). A high-pressure region (a stagnation point could arise if there is significant inflow) forms momentarily near the trailing edge of the cavity. The transient nature of the flow causes the emission of a compression wave. The compression wave propagates in all directions. The shape of the wave front will, of course, be modified by the convection effect of the mean flow as it radiates away from the trailing edge of the cavity. This model differs significantly from the unsteady mass addition and removal model

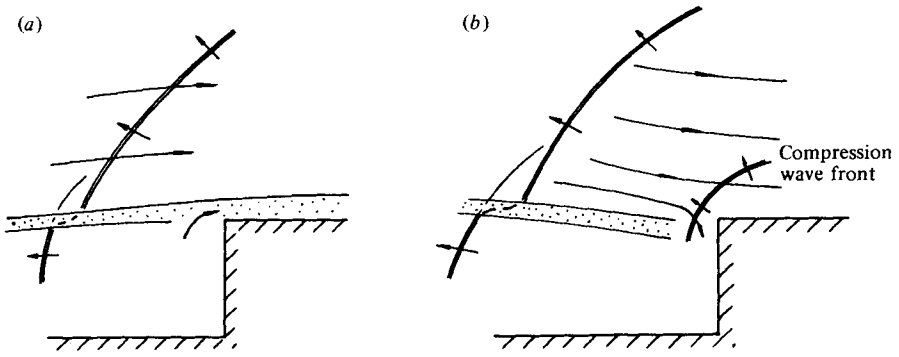

FIGURE 6. (*a*) Shear layer deflecting upward – external fluid flows smoothly over trailing edge of cavity. (*b*) Shear layer deflecting downward – external flow impinges on trailing edge of cavity producing compression wave.

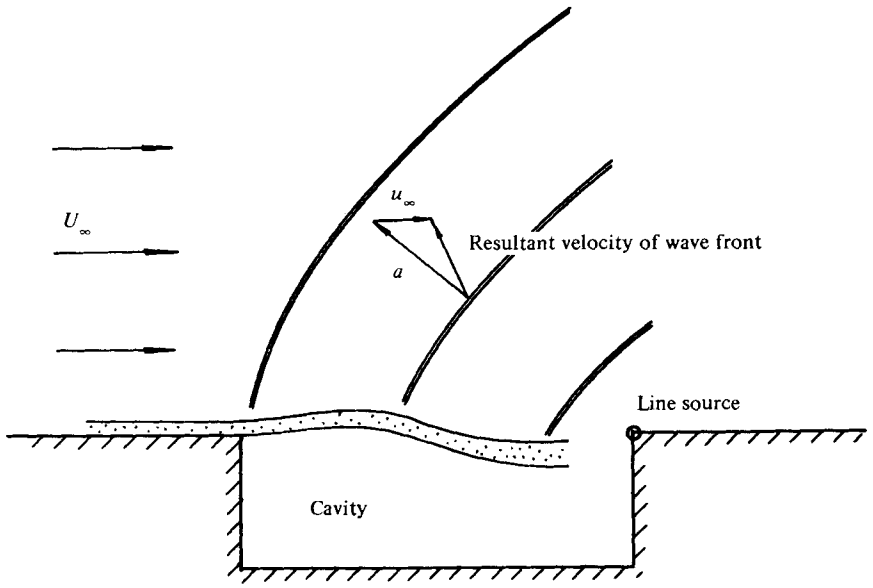

FIGURE 7. Acoustic wave pattern outside the cavity.

of Bilanin & Covert. Unlike the Bilanin & Covert model, the present model is consistent with the visual observations of Krishnamurty (1955) and Heller & Bliss (1975).

For the purpose of computing the phases of the acoustic waves generated at the trailing edge of the cavity, the effective size of the noise source can be regarded as very small. Krishnamurty (1955) and later Spee (1966) obtained schlieren pictures of the acoustic wave field outside the cavity. By assuming that the waves were produced by a periodic line source at the trailing edge of the cavity and accounting only for the convection effect of the mean flow and the propagation velocity of sound (i.e. a periodic line source in an uniform flow of infinite extent), they were able to construct theoretically (see figure 7) the wave fronts of the emitted pressure waves. These pictures look remarkably close to those obtained experimentally, indicating that a periodic line source approximation is reasonable. As a result of these observations,

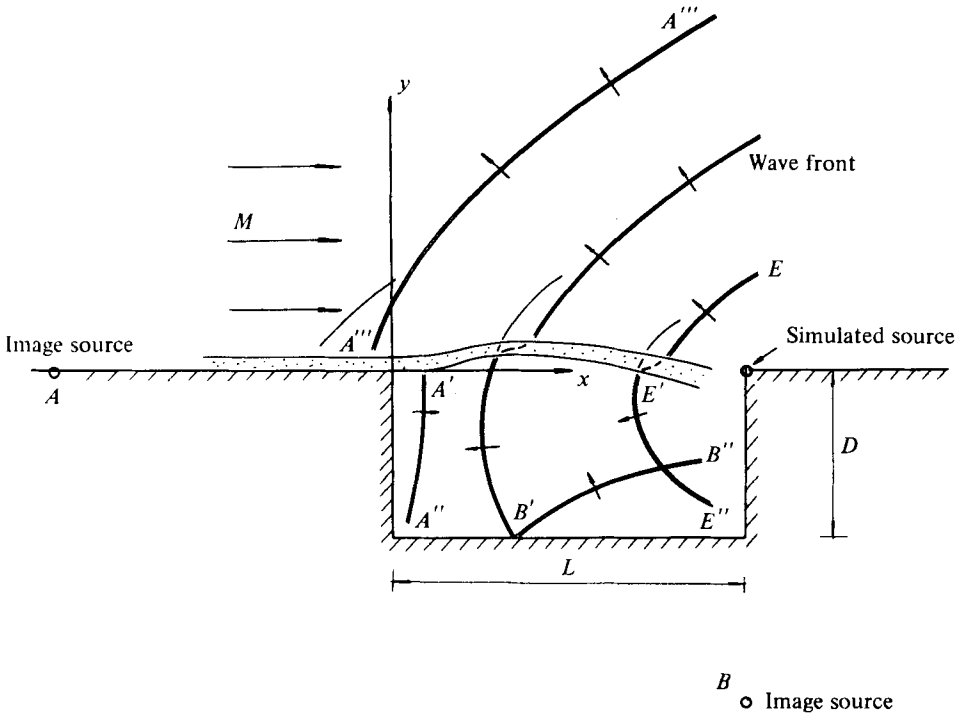

FIGURE 8. Acoustic wave field inside and outside rectangular cavity.

the wave pattern produced by a periodic line source located at the trailing edge of the cavity will be used in the present model to simulate the real wave field. Inside the cavity the same approximation will be used. Here, of course, the mean velocity is zero. Let p_{d+} and p_{d-} represent the pressure field generated outside and inside the cavity respectively by the aforementioned trailing-edge interaction process. Then, with respect to the co-ordinate system as shown in figure 8 (see Gottlieb 1960), one finds that

$$\left.\begin{aligned} p_{d+}(x,y,t) &= \frac{Q}{2\pi} H_0^{(1)}\left[\frac{\omega}{a_+(1-M^2)^{\frac{1}{2}}}\left(\frac{(x-L)^2}{1-M^2}+y^2\right)^{\frac{1}{2}}\right]\exp\left[i\frac{\omega M(L-x)}{a_+(1-M^2)}-i\omega t\right], \\ & \qquad\qquad y \geqslant 0, \\ p_{d-}(x,y,t) &= \frac{Q}{2\pi} H_0^{(1)}\left[\frac{\omega}{a_-}((L-x)^2+y^2)^{\frac{1}{2}}\right]\exp(-i\omega t), \quad y \leqslant 0 \end{aligned}\right\} \tag{1}$$

(subscript d denotes radiated pressure field), where $H_0^{(1)}$ is the zeroth-order Hankel function of the first kind, ω is the angular frequency of oscillation, a_+ and a_- are the speeds of sound outside and inside the cavity respectively, $M = \bar{U}_\infty/a_+$ is the Mach number, $\bar{U}_\infty$ is the speed of external flow and Q is the source strength. In (1), the expression for p_{d+} satisfies the convective wave equation and p_{d-} is a solution of the simple wave equation. p_{d+} is equal to zero for supersonic flows. The value Q in the expressions is related to the displacement of the shear layer ζ at the trailing edge of the cavity.

Since the trailing edge of the cavity is most exposed to the external flow when the shear layer is deflected to its maximum position inside the cavity, it is expected that the pressure near the line source is highest under these circumstances. Now for $x \to L$, the pressure field as given by (1) becomes

$$p \to -\frac{iQ}{2\pi}\left|\ln\left(\frac{\omega\epsilon}{a}\right)\right| \exp(-i\omega t), \tag{2}$$

$$x \to L-\epsilon,$$

$$\epsilon \ll 1.$$

If $\zeta(x,t)$ is equal to $\hat{\zeta}(x)\exp(-i\omega t)$, then the above reasoning (i.e. p attains a positive maximum value when $\zeta(L,t)$ is most negative) provides the following phase relationship between $\hat{\zeta}(L)$ and Q:

$$\hat{\zeta}(L) = iQ\kappa, \tag{3}$$

where κ is an as yet unknown positive real constant. It turns out it is possible to determine the cavity tone frequencies without knowing the exact value of κ. For this reason no attempt will be made to estimate its value.

Since the compression waves generated at the trailing edge of the cavity radiate in all directions, the part which is radiated into the external flow will propagate to infinity without suffering any reflexion as shown in figure 8. The part of the waves which is radiated into the cavity, e.g. wave front $E'E''$, will be reflected by the bottom wall and the upstream end wall of the cavity. These reflexions give rise to wave fronts $B'B''$ and $A'A''$ as indicated in figure 8. Further reflexions of the waves by the walls of the cavity and the shear layer are inevitable. However, a careful study of the visualization results of Heller & Bliss (1975) reveal that reflexions from the shear layer and subsequent reflexions from the cavity walls are negligibly weak compared with those mentioned above when feedback oscillations occur. For simplicity, therefore, secondary reflexions will be ignored in the present model. The directly radiated wave EE' and the reflected waves $A'A''$ and $B'B''$ all tend to excite the instability waves of the shear layer. It turns out that the excitation due to reflected waves $A'A''$ is most important. To calculate their effect on the shear layer, the wave field BB' can be simulated by using a periodic line image source B located at $x = L, y = -2D$ as shown in figure 8. Similarly, the reflected wave field $A'A''$ can be simulated by means of an image line source A at $x = -L$, $y = 0$. The pressure and velocity field due to these image line sources are

$$\left.\begin{aligned} p_r(x,y,t) = \frac{Q}{2\pi}\left\{H_0^{(1)}\left[\frac{\omega}{a_-}((x+L)^2+y^2)^{\frac{1}{2}}\right]\right. \\ \left. + H_0^{(1)}\left[\frac{\omega}{a_-}((L-x)^2+(y+2D)^2)^{\frac{1}{2}}\right]\right\}\exp(-i\omega t), \end{aligned}\right\} \tag{4}$$

$$v_r(x,y,t) = \frac{i}{\rho_-\,\omega}\frac{\partial p_r}{\partial y}, \qquad y \leqslant 0 \tag{5}$$

(subscript r denotes the reflected acoustic field). In (5), v_r is the velocity component in the direction of y and ρ_- is the density of fluid inside the cavity.

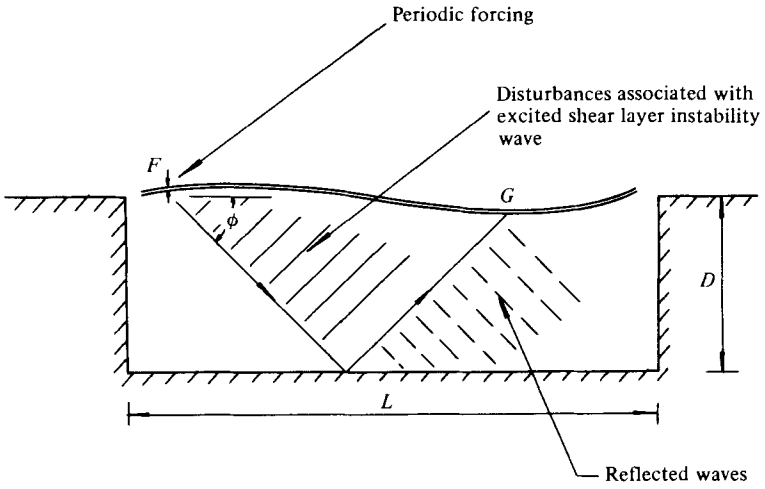

FIGURE 9. Reflexion by bottom wall of cavity.

To complete the mathematical model it is necessary to determine the effect of the interaction of the acoustic wave field (both the directly radiated field and the reflected field) on the instabilities of the shear layer. It is known from previous work (Tam 1971) that the instability waves involved are of the convective type. That is to say, the unstable waves have negligible upstream influence [see also (16) below]. This is important for it allows one to treat the shear layer as infinite in extent without incurring substantial error. Also, it is known experimentally that the bottom wall of the cavity (except for very shallow ones) does not interfere with the motion of the free shear layer. To estimate the effect of the cavity bottom wall on the acoustically excited instability characteristics of the shear layer one can make use of the solution obtained by Tam (1971). Tam's solution shows that the disturbance generated by periodically excited shear layer instability is confined mainly to a sector making an angle ϕ to the downstream direction as shown in figure 9. The principal effect of the bottom wall is to reflect this disturbance upward towards the shear layer. For the present purpose, it seems reasonable to assume that the incident and the reflected angles of the incident and reflected waves be the same relative to the normal to the bottom wall. From figure 9 it is clear that the reflected waves will not be able to reach the shear layer directly to excite it unless the length of the cavity L is greater than $2D\cot\phi$. The angle ϕ is not too sensitive to the flow Mach number. It varies from 45° at $M = 0{\cdot}2$ to 41° at $M = 2{\cdot}0$. Therefore, on ignoring secondary reflexions one finds that the bottom wall of the cavity has little effect on the excited shear layer instability for cavities with aspect ratio $L/D < 2$. For cavities with L somewhat greater than $2D$ the directly reflected waves (bottom wall) will reach the shear layer and excite it. When this happens, however, the amplitude of the excited instability wave must be small compared with the original excited instability wave, which has grown by a factor $\exp(-2k_iD)$ on propagating over the distance FG (see figure 9), where $-k_i$ is the growth rate of the instability wave. Thus taking these factors into account and for reasons of simplicity, the presence of the bottom cavity wall is ignored as far as computing the instability characteristics of the shear layer is concerned. Figure 10 shows the model to be used for the purpose of computing the excitation of shear layer

instability waves by an acoustic field. Here, of course, the pressure and velocity loading on the shear layer is restricted to the interval $x = 0$ to $x = L$. From (1), (4) and (5), these loadings are

$$\left.\begin{aligned}\Delta p &= p(x, y = 0^-, t) - p(x, y = 0^+, t) \equiv \Delta\hat{p}(x)\exp(-i\omega t),\\ \Delta v &= v(x, y = 0^-, t) \equiv \Delta\hat{v}(x)\exp(-i\omega t),\end{aligned}\right\} \tag{6}$$

where

$$\left.\begin{aligned}\Delta\hat{p}(x) &= \frac{Q}{2\pi}\left\{H_0^{(1)}\left[\frac{\omega}{a_-}(L-x)\right] - H_0^{(1)}\left[\frac{\omega(L-x)}{a_+(1-M^2)}\right]\exp\left[i\frac{\omega M(L-x)}{a_+(1-M^2)}\right]\right.\\ &\quad\left. + H_0^{(1)}\left[\frac{\omega}{a_-}(x+L)\right] + H_0^{(1)}\left[\frac{\omega}{a_-}((L-x)^2+4D^2)^{\frac{1}{2}}\right]\right\},\\ \Delta\hat{v}(x) &= \frac{Q}{2\pi\rho_- a_-}\frac{i2D}{[(L-x)^2+4D^2]^{\frac{1}{2}}}H_1^{(1)}\left[\frac{\omega}{a_-}((L-x)^2+4D^2)^{\frac{1}{2}}\right],\end{aligned}\right\} \tag{7}$$

for $$0 \leqslant x \leqslant L.$$

In (7), $H_1^{(1)}$ is the first-order Hankel function of the first kind. A thin vortex model of the shear layer will first be used to develop an analytical expression for the excited amplitude and phase of the unstable waves. A correction for finite shear layer thickness effect will be made in the next section of this paper.

The shear layer of an oscillating cavity is generally turbulent. Thus the present problem involves the modelling of the excitation of unstable waves of a turbulent shear layer by sound. Recently, a good deal of work has been carried out on this particular subject using hydrodynamic stability theory. Chan (1974*a*, *b*, 1976, 1977) and Moore (1977), in a series of theoretical and experimental studies involving the turbulent shear layer of jets, found that hydrodynamic stability calculations on wave speeds as well as local growth rates agreed quite well with measurements. This is true not only for plane wave excitation but also for higher-order wave modes. In this paper we follow the works of Chan and Moore and formulate the excitation problem within the framework of hydrodynamic stability theory.

To solve the mathematical problem as posed it is convenient first to construct the appropriate Green's function. For a thin shear layer subjected to pressure and velocity loading at a point $x = \xi$ the governing equation and boundary conditions are

$$\left.\begin{aligned}\frac{1}{a_+^2}\left(\frac{\partial}{\partial t}+\overline{U}_\infty\frac{\partial}{\partial x}\right)^2 p_+ - \nabla^2 p_+ &= 0, &(8)\\ \rho_+\left(\frac{\partial v_+}{\partial t}+\overline{U}_\infty\frac{\partial v_+}{\partial x}\right) &= -\frac{\partial p_+}{\partial y}, &(9)\end{aligned}\right\} \quad y \geqslant 0,$$

$$\left.\begin{aligned}\frac{1}{a_-^2}\frac{\partial^2 p_-}{\partial t^2} - \nabla^2 p_- &= 0, &(10)\\ \rho_-\frac{\partial v_-}{\partial t} &= -\frac{\partial p_-}{\partial y}, &(11)\end{aligned}\right\} \quad y \leqslant 0.$$

As $y \to \pm\infty$ disturbances are bounded. At $y = 0$,

$$\left(\frac{\partial}{\partial t}+\overline{U}_\infty\frac{\partial}{\partial x}\right)\eta = v_+, \tag{12}$$

$$\frac{\partial\eta}{\partial t} = v_- + A\delta(x-\xi)\exp(-i\omega t), \tag{13}$$

$$p_+ = p_- + B\delta(x-\xi)\exp(-i\omega t) \tag{14}$$

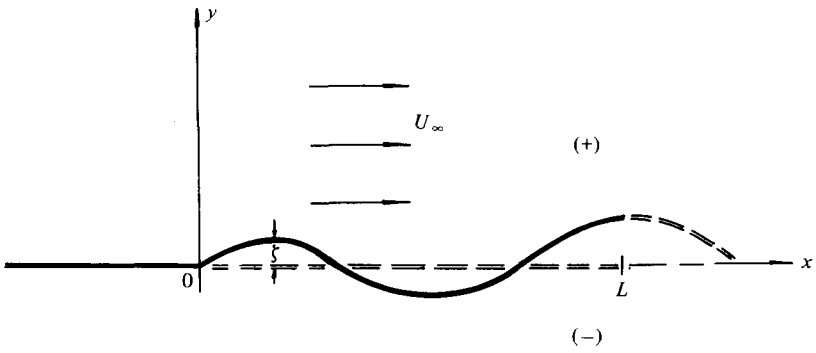

FIGURE 10. Vortex sheet subjected to pressure and velocity loading from $x = 0$ to $x = L$.

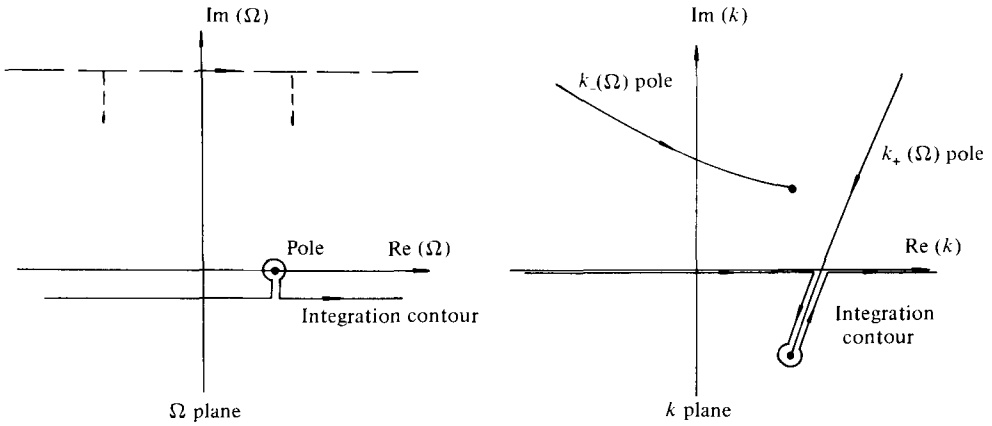

FIGURE 11. Complex k and Ω planes showing poles and inverse contours. Branch cuts are not shown.

(A, B are constants; $\delta(x)$ is the Dirac delta function), where p, v, ρ and η denote the pressure, velocity component in the y direction, fluid density and the displacement of the shear layer respectively. The subscript + or − indicates whether the physical quantity under consideration is associated with the moving or stationary medium as in figure 10.

A simplified version of the above problem, namely with $A = 0$, was solved by Tam (1971), by means of the Fourier–Laplace transform technique. To evaluate the inverse transforms in the appropriate complex plane, a procedure developed by Briggs (1964) was employed. The solution of the present mathematical problem can be constructed in the same way. It is straightforward to find that $\eta(x, t)$, the displacement of the shear layer, is given by

$$\eta(x,t) = \frac{1}{4\pi^2}\int_{-\infty+i\sigma}^{+\infty+i\sigma}\int_{-\infty}^{\infty} \frac{(i\beta_+\beta_- B - \rho_-\Omega\beta_+ A)\exp[ik(x-\xi)-i\Omega t]}{\Delta(k,\Omega)(\Omega-\omega)}\,dk\,d\Omega, \qquad (15)$$

where

$$\Delta(k,\Omega) = \rho_+ a_+^2(\beta_- + \beta_+)(k^2 - \beta_+\beta_-),$$

$$\beta_+ = \left[k^2 - \frac{1}{a_+^2}(\Omega - \bar{U}_\infty k)^2\right]^{\frac{1}{2}}, \quad \mathrm{Re}\,(\beta_+) < 0,$$

$$\beta_- = [k^2 - \Omega^2/a_-^2]^{\frac{1}{2}}, \quad \mathrm{Re}\,(\beta_-) < 0.$$

The complex integrals of (15) are to be evaluated by first allowing σ to be very large and positive so that the inverse contour is above all poles in the complex Ω plane as shown in figure 11. It is shown (see Tam 1971) that there are two poles, namely $k_+(\Omega)$ and $k_-(\Omega)$, in the k plane. They are the zeros of $\Delta(k, \Omega)$. On deforming the inverse contour in the Ω plane towards the real axis, the $k_+(\Omega)$ pole crosses the real axis in the complex k plane as depicted in figure 11. It is this pole which gives rise to an amplifying (unstable) wave solution in the positive x direction. On picking up the contribution from the pole at $\Omega = \omega$ in the Ω plane and the pole $k = k_+(\omega)$ in the k plane, one readily finds that the displacement of the shear layer associated with the unstable wave solution is

$$\eta(x,t) = \begin{cases} \left.\dfrac{i\beta_+\beta_- B - \rho_-\omega\beta_+ A}{\partial\Delta/\partial k} \exp\left[ik_+(x-\xi) - i\omega t\right]\right|_{k=k_+(\omega),\,\Omega=\omega} & ; \quad (x-\xi) > 0, \\ 0 & ; \quad (x-\xi) < 0, \end{cases} \tag{16}$$

It is to be noted that (16) is not the full result of (15). It is, however, the part of η associated with the unstable wave as excited by the inhomogeneous terms of (13) and (14). The contributions from the remaining part of the contour in the k plane which gives rise to η associated with the transmitted or reflected wave of the vortex sheet (see Gottlieb 1960) and the contribution from the k_- pole and others are of no immediate interest to the present problem and are, therefore, disregarded. By means of (16) the displacement of the shear layer, ζ, due to Δp and Δv of (6) and (7) can easily be found:

$$\left.\begin{aligned} \zeta(x,t) = {} & \frac{i\beta_+\beta_-}{\left(\dfrac{\partial\Delta}{\partial k}\right)}\Bigg|_{k=k_+(\omega)} \int_0^L \Delta\hat{p}(\xi)\exp\left[ik_+(x-\xi)\right]H(x-\xi)\,d\xi\exp\left[-i\omega t\right] \\ & -\rho_-\omega\frac{\beta_+}{\left(\dfrac{\partial\Delta}{\partial k}\right)}\Bigg|_{k=k_+(\omega)} \int_0^L \Delta\hat{v}(\xi)\exp\left[ik_+(x-\xi)\right]H(x-\xi)\,d\xi\exp\left[-i\omega t\right]. \end{aligned}\right\} \tag{17}$$

In (17), $H(z)$ is the unit step function. The displacement of the shear layer at the trailing edge of the cavity is determined by putting $x = L$ in (17). Upon invoking the phase relationship between $\hat{\zeta}(L)$ and Q as given by (3) the following expression is obtained:

$$\kappa = \psi(\omega L/\bar{U}_\infty, M, L/D), \tag{18}$$

where

$$\left.\begin{aligned} \psi(\omega L/\bar{U}_\infty, M, L/D) = {} & \frac{1}{2\pi}\frac{\beta_+\beta_-}{\left(\dfrac{\partial\Delta}{\partial k}\right)}\Bigg|_{k=k_+(\omega)} \exp\left(ik_+L\right)\int_0^L \Bigg\{H_0^{(1)}\left[\frac{\omega}{a_-}(L-\xi)\right] \\ & - H_0^{(1)}\left[\frac{\omega}{a_+}\frac{(L-\xi)}{(1-M^2)}\right]\exp\left[i\frac{\omega M(L-\xi)}{a_+(1-M^2)}\right] + H_0^{(1)}\left[\frac{\omega}{a_+}(\xi+L)\right] \\ & + H_0^{(1)}\left[\frac{\omega}{a_-}((L-\xi)^2+4D^2)^{\frac{1}{2}}\right] - \frac{\omega}{a_-\beta_-}\frac{2D}{((L-\xi)^2+4D^2)^{\frac{1}{2}}} \\ & \times H_1^{(1)}\left[\frac{\omega}{a_-}((L-\xi)^2+4D^2)^{\frac{1}{2}}\right]\Bigg\}\exp\left(-ik_+\xi\right)d\xi. \end{aligned}\right\} \tag{19}$$

In this way the feedback loop is closed. The left-hand side of (18) is real; hence the phase of ψ must be equal to an integral multiple of 2π, i.e.

$$\text{phase of } \psi = 2\pi n; \quad n = 1, 2, 3, \ldots . \tag{20}$$

Equation (20) is not satisfied in general unless the Strouhal number $fL/\bar{U}_\infty$ (where $2\pi f = \omega$) of the cavity acoustic oscillation takes on certain special values. For a given flow Mach number M and cavity length to depth ratio L/D these are the discrete oscillation frequencies. Equations (19) and (20) can be computed numerically. The predicted oscillation frequencies will be used to compare with experimental measurements in a later section of this paper.

3. The effect of finite shear layer thickness

The mathematical model of §2 assumed the shear layer which spans the mouth of the cavity to have negligible thickness. This approximation turns out to be not very accurate. For instance, in Rossiter's experiment (1964), the boundary-layer thickness δ was approximately 0·65 in. at subsonic speeds. The length L of the cavities used was 8 in., giving a ratio $\delta/L = 0{\cdot}081$ which is not completely negligible (under this condition δ/wavelength of the unstable wave is also not negligible especially for the higher-order tones such as $n = 3, 4$). Actually it is believed that the scatter of the data in figure 5 is due primarily to variations in the initial shear layer thickness of the different experiments. Linear instability analysis of two-dimensional mixing layers, e.g. Michalke (1965), shows that the phase speeds or the dispersion relation $k = k_+(\omega)$ of instability waves of a given frequency depends very much on the shear layer thickness. In order to predict the cavity tone frequencies accurately a good estimate of the dispersion relation or phase speed is vital as can be seen in (19). Here it is proposed to correct for the thickness effect of the present model by substituting the relationship $k_+(\omega, \theta)$ as obtained for a shear layer of finite momentum thickness θ in (19) and (20) instead of the value obtained from the dispersion relation of a thin vortex sheet. This modification to (20) leads to the following eigenvalue formula for predicting the discrete tone frequencies:

$$\text{phase of } \psi(\omega L/\bar{U}_\infty, M, L/\theta, L/D) = 2\pi n; \quad n = 1, 2, 3, \ldots . \tag{21}$$

Because of entrainment, the thickness of the shear layer increases in the downstream direction. The spatial rate of growth of the shear layer thickness on the other hand depends on the amplitude of cavity oscillation. These processes are interrelated and not fully understood at the present time. For the purpose of making a reasonably accurate estimate of the cavity tone frequencies it is feasible, therefore, only to take the thickness effect into account in an averaged sense. It will be assumed that the shear layer can be characterized by a mean momentum thickness θ throughout its entire length. The mean velocity profile of the cavity shear layer has never been measured in any such detailed way as to be useful. In the absence of this information, the mean flow profile is taken to be the same as that of a two-dimensional free turbulent mixing layer near the trailing edge of a thin flat plate. The latter is readily available in the work of Liepman & Laufer (1974), Wygnanski & Fiedler (1970), Patel

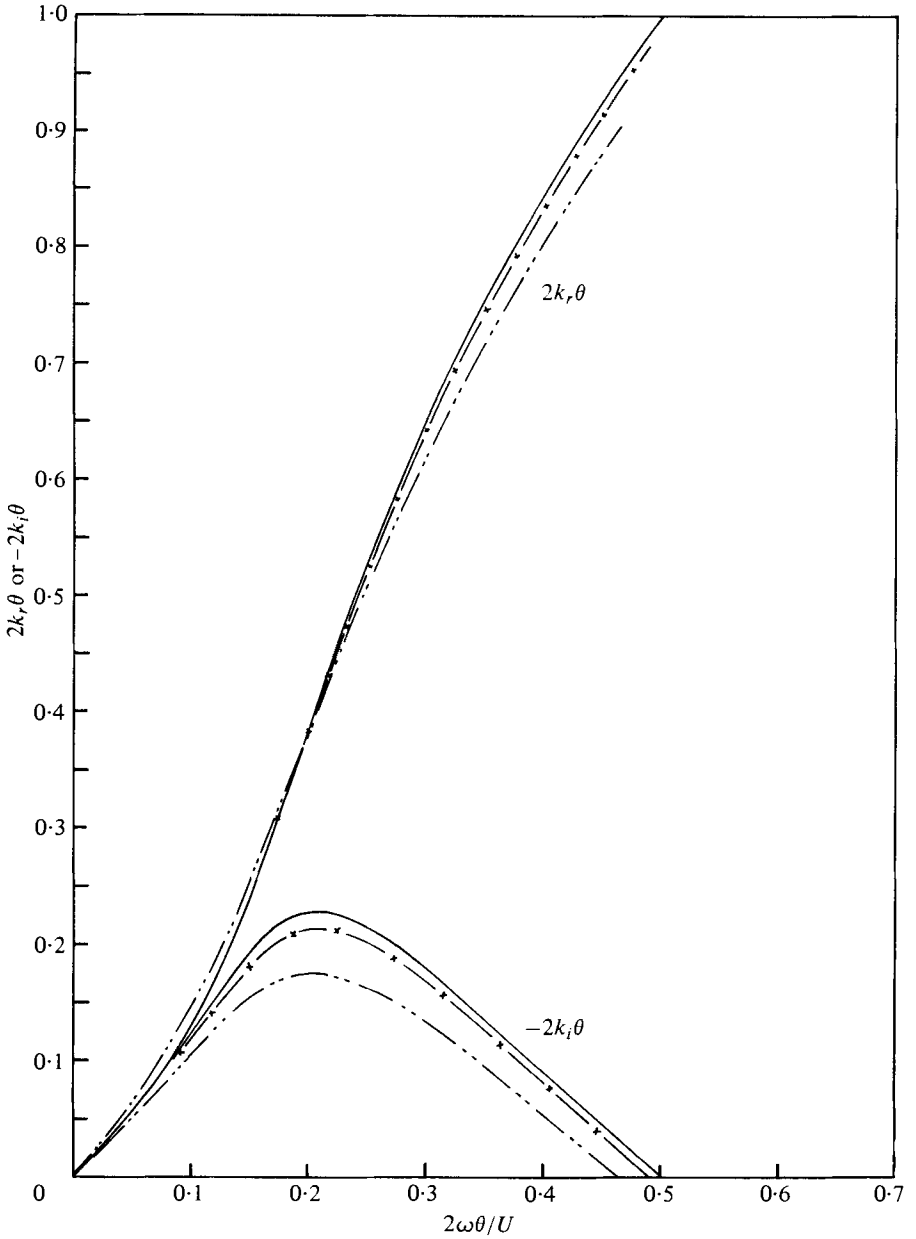

FIGURE 12. Instability characteristics of shear layer.
—·—·—, $M = 0{\cdot}8$; ×—×, $M = 0{\cdot}4$; ——, $M = 0{\cdot}0$.

(1973), Champagne, Pao & Wygnanski (1976) and others. The following simple analytical expression seems to fit the experimental measurements very well:

$$\overline{U}(y) = \frac{\overline{U}_\infty}{2}\left(1+\tanh\left(\frac{y}{2\theta}\right)\right). \tag{22}$$

In (22), θ is the momentum thickness of the shear layer. This profile will be used in determining $k_+(\omega, M, \theta, U_\infty)$.

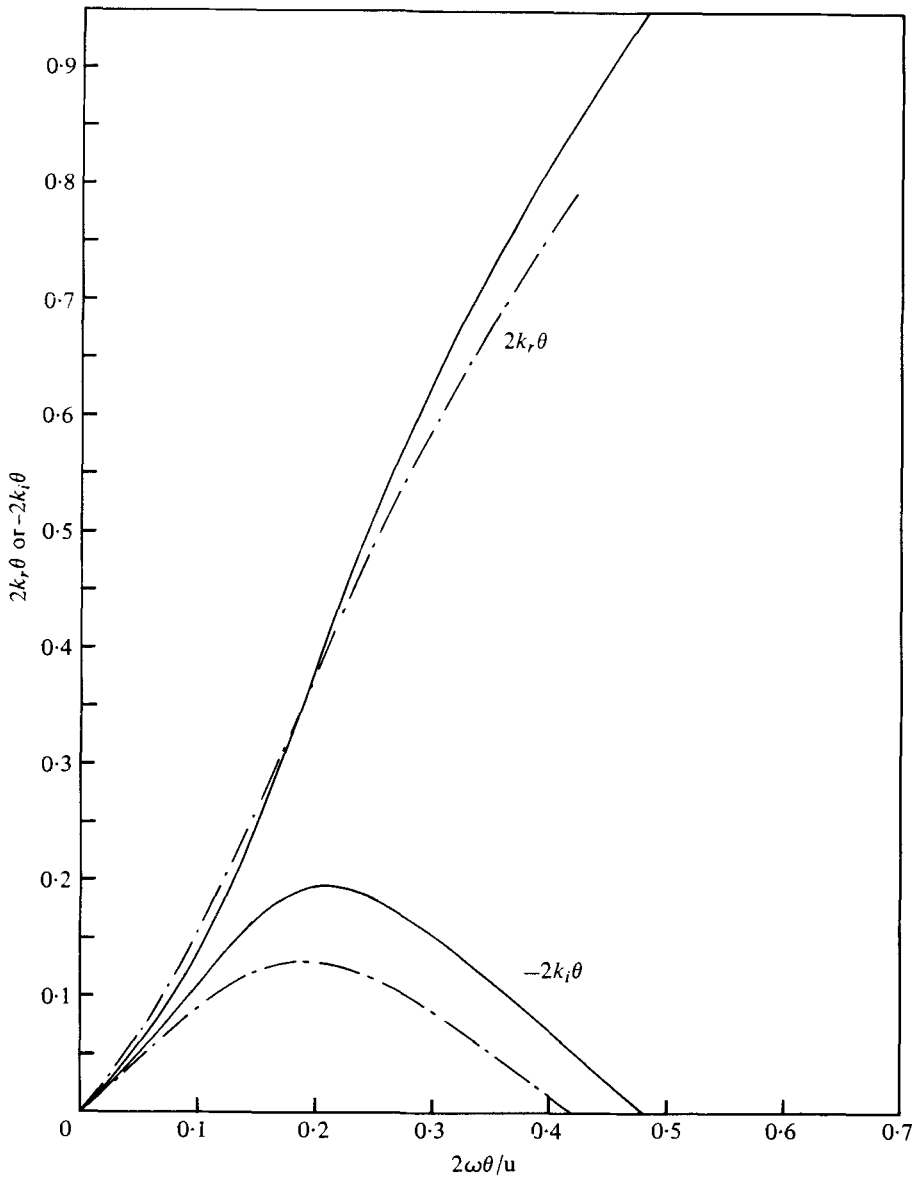

FIGURE 13. Instability characteristics of shear layer.
——, $M = 0{\cdot}6$; —·—, $M = 1{\cdot}2$.

Let $p(x, y, t) = \hat{p}(y) \exp[i(k_+ x - \omega t)]$ be the pressure disturbance associated with the shear layer instability wave. Then, following standard linear hydrodynamic stability theory, e.g. Lin (1955), Michalke (1965), the equation for $\hat{p}(y)$ is

$$\frac{d^2\hat{p}}{dy^2} + \left[\frac{2k_+}{(\omega - k_+\bar{U})}\frac{d\bar{U}}{dy} - \frac{1}{\bar{\rho}}\frac{d\bar{\rho}}{dy}\right]\frac{d\hat{p}}{dy} + \left[\frac{(\omega - \bar{U}k_+)^2}{\bar{a}^2} - k_+^2\right]\hat{p} = 0. \tag{23}$$

In deriving (23), the inviscid parallel flow assumptions were used. To specify the mean density $\bar{\rho}$, the mean speed of sound $\bar{a}$, the total temperature and mean pressure of the

flow will be regarded as constant across the shear layer. This gives

$$\left(\frac{\bar{a}}{a_\infty}\right)^2 = 1+\frac{\gamma-1}{2}M^2\left[1-\left(\frac{\bar{U}}{\bar{U}_\infty}\right)^2\right],$$

$$\frac{\bar{\rho}}{\rho_\infty} = \left(\frac{a_\infty}{\bar{a}}\right)^2,$$

where a_∞, ρ_∞ are the sound speed and mean density of the external flow outside the shear layer, M is the external flow Mach number and γ is the ratio of specific heats. Equation (23) together with the boundedness condition at $y \to \pm\infty$ forms an eigenvalue problem by which $k_+(\omega, M, \theta, \bar{U}_\infty)$ can be determined. This problem can easily be solved numerically. Figures 12 and 13 show typical values of real and imaginary parts of k_+ ($k_+ = k_r + ik_i$) as functions of $2\omega\theta/\bar{U}_\infty$ for various Mach numbers over the whole unstable frequency range. These numerical results were obtained using the computing facility of the N.A.S.A. Langley Research Center. To facilitate the computation of (19) and (21), the numerical values of $2\theta k_+$ for a given Mach number are fed into a cubic spline curve fit computer program subroutine. In this way the numerical values of k_+ for any unstable frequency are readily available.

4. Experimental arrangement and procedure

The cavity used to generate data for comparison purposes was designed to have a continuously variable streamwise length (0–24 cm) and a depth which varied in two steps, 3·19 and 5·11 cm. The latter was accomplished by sliding blocks as shown in figure 14. Four cavity configurations that were tested are listed below:

Length, L (cm)	Depth, D (cm)	L/D
4·0	5·11	0·783
12·0	5·11	2·348
2·5	3·193	0·783
7·5	3·193	2·348

The cavity was 5·08 cm wide.

The apparatus was constructed of tempered, 1·25 cm thick aluminium barstock. The above cavity was set in a 1·25 cm thick tempered aluminium plate which was curved downstream of the cavity to reduce any trailing-edge noise. The plate was flush with the lower lip of a 30 by 45 cm nozzle. The nozzle exit velocity varied from a Mach number of 0·05 to 0·40. The maximum shear layer thickness δ at the cavity leading edge was approximately 0·76 cm at Mach number 0·4. The experiment was performed in the A.N.R.L. open jet anechoic flow facility at the N.A.S.A. Langley Research Center, Hampton, Virginia.

The acoustic data were obtained with a $\frac{1}{2}$ in. condenser-type microphone which was located 2·13 m above the cavity as noted in figure 15. The data acquisition system consisted of a pre-amplifier, power supply, filter, amplifier, and spectrum analyser. The spectrum analyser was capable of identifying the frequency of the tones in the radiated noise spectrum of the cavity to within 10 Hz. This allowed sufficiently accurate determination of the frequency which was used to calculate the Strouhal number ($fL/\bar{U}_\infty$).

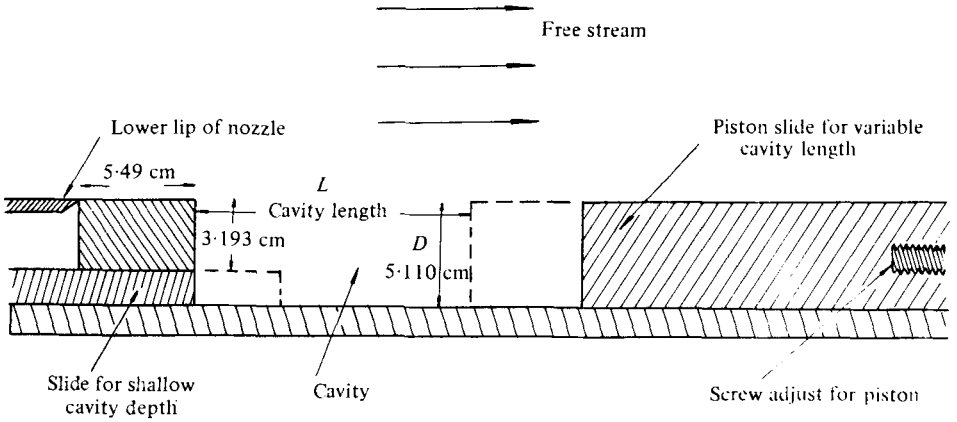

FIGURE 14. Cross-section of cavity.

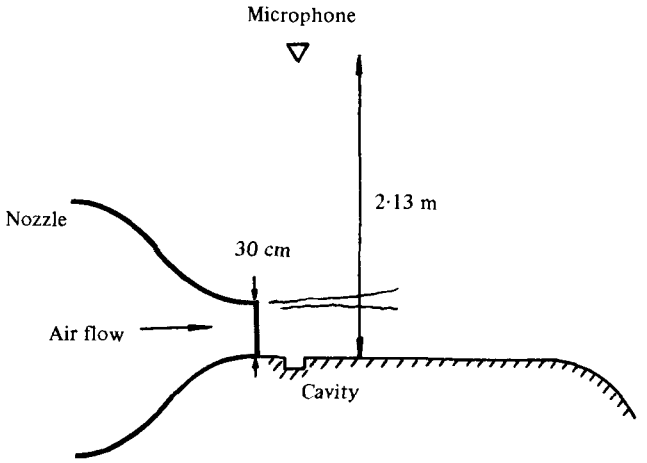

FIGURE 15. Cavity in A.N.R.L. open jet anechoic flow facility.

The following procedure was used to obtain the Strouhal number as a function of Mach number. The cavity dimensions were fixed yielding a particular value of L/D. The two values of L/D used in this experiment (as shown in the above table) were 0·783 for a fairly deep cavity and 2·35 for a shallow cavity. After the L/D value was set, the Mach number was varied in small increments from $M = 0{\cdot}05$ to 0·40. The frequencies of the radiated tones were recorded. The cavity dimensions were then adjusted to give the same value of L/D with a differing cavity dimension and the process was repeated. About 300 data points were generated.

5. Comparison between theory and experiment

The measured discrete tone frequencies as a function of Mach number are shown in figures 16 and 18. As can readily be seen in figure 16 for shallow cavities, the tone frequencies fall into bands in the Strouhal number $fL/\bar{U}_\infty$ versus Mach number M plot for Mach numbers greater than 0·2 in the case of the smaller cavity and 0·12 in

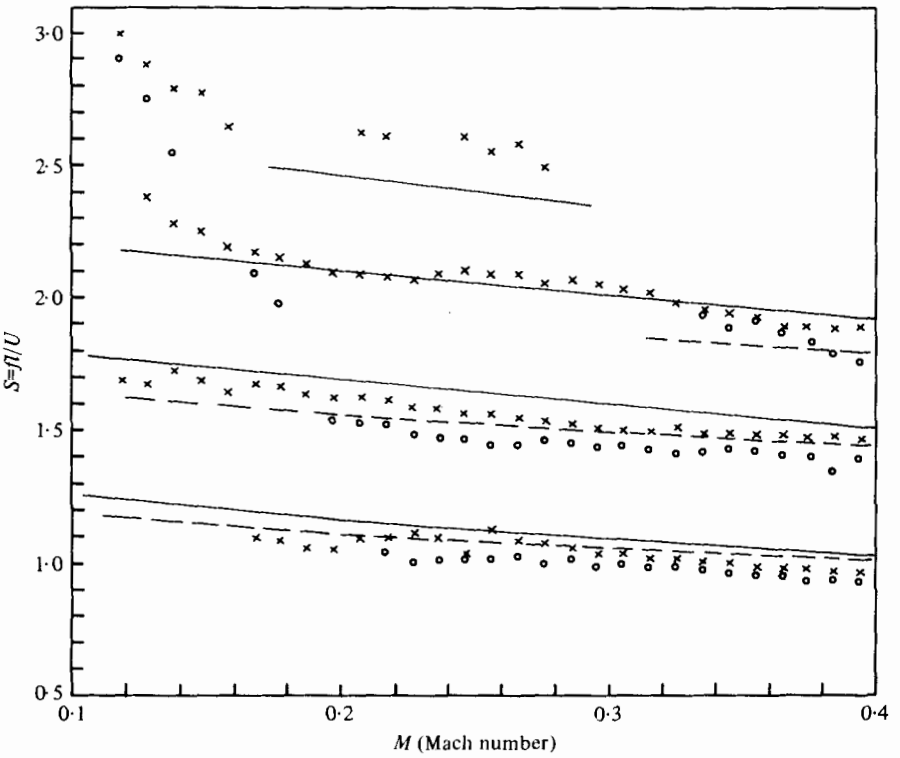

FIGURE 16. Discrete tone frequencies as a function of Mach number. ×, L = 12 cm, D = 5·08 cm, L/D = 2·36; ○, L = 7·5 cm, D = 3·175 cm, L/D = 2·36. Theoretical, equations (21) and (19): ——, $L/2\theta$ = 90; — —, $L/2\theta$ = 70.

the case of the larger cavity. For deep cavities only one discrete tone frequency (excluding harmonics) was found over most of the Mach number range of the experiments (see figure 18). For these cavities, the dependence of tone Strouhal number on Mach number at Mach numbers less than 0·2 is distinctly different from that for higher Mach numbers, suggesting that the tones are probably generated by an entirely different mechanism. This question will be discussed further in the later part of this section.

In §§2 and 3, a model of the cavity feedback oscillation mechanism was proposed. Here comparison between the theoretically predicted cavity tone frequencies of this model, namely (19) and (21), and experimental measurements will be made. In the theoretical model, the Strouhal numbers of the discrete tones depend on the parameter $L/2\theta$, where L is the length of the cavity and θ is the averaged momentum thickness of the shear layer. Since θ is not measured in most experiments, an approximate but reasonable value of this parameter will be used. In Rossiter's (1964) experiment the initial turbulent boundary-layer thickness δ upstream of the cavity was 0·65 in. at subsonic speeds and 0·55 in. at M = 1·2. The cavities used in the experiments had a length L of 8 in. On assuming that the turbulent boundary-layer flow had a $\frac{1}{7}$ power velocity distribution as in the case of a smooth flat plate [see Schlichting (1960), chapter 11], then the momentum thickness θ and the boundary-layer thickness δ are related by $\theta = \frac{7}{72}\delta$. By means of this formula and on taking into account the fact

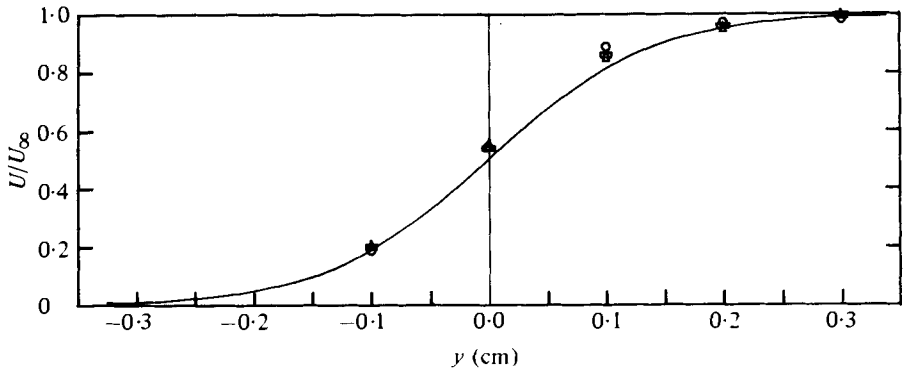

FIGURE 17. Mean velocity profile of shear layer at 0·9 cm downstream of leading edge of cavity. L = 12 cm. ○, U_∞ = 50·0 m/s; □, U_∞ = 84·4 m/s; △, U_∞ = 124·2 m/s; ——, equation (22) with $L/2\theta$ = 90.

that the averaged momentum thickness θ of the shear layer must be somewhat larger than that of the initial turbulent boundary layer, it seems reasonable, therefore, to assume $L/2\theta$ to be 50 in Rossiter's experiments. The solid curves of figure 19 show the predicted Strouhal numbers of cavity tones as functions of Mach number for $L/D = 4$, $L/2\theta = 50$ over the Mach number range of $0{\cdot}4 \leqslant M \leqslant 1{\cdot}2$. These curves are to be compared with Rossiter's experimental data also shown in this figure. On considering that the theoretical curves are without any adjustable constant while the measurements have some degree of uncertainty it is deemed that the agreement is favourable. Figure 16 gives a comparison of the predicted and experimentally measured tone Strouhal numbers versus flow Mach numbers over the low subsonic Mach number range of 0·1–0·4 for shallow cavities. In the theoretical model, $L/2\theta$ was taken to be 90 and $L/D = 2{\cdot}36$. The predicted values (solid curves) seem to agree quite well with the observed Strouhal numbers for the larger cavity. The value of $L/2\theta$ was estimated by fitting (22) to the measured mean velocity profile. This is shown in figure 17. The mean flow data were taken at a point 0·9 cm downstream of the leading edge of the cavity. In this figure $y = 0$ is at the same level as the top of the cavity. From these measurements it is observed that for a given cavity the parameter $L/2\theta$ is quite constant over the Mach number range of 0·15–0·4. Thus the dependence of this parameter on Mach number will be ignored in the present calculations. For the small cavity, $L/2\theta$ is smaller and the value $L/2\theta$ is estimated to be 70. The calculated tone Strouhal number versus Mach number curves for $L/2\theta = 70$ are plotted (dotted curves) in figure 16. The agreement between theoretical and measured tone frequencies, as can be seen, is quite good. It is important to point out that, even though L/D is the same for both cavities, the tone Strouhal number at a given flow Mach number is consistently somewhat smaller for the smaller cavity than for the larger one. The implication is that L/θ is also an important parameter of the tone frequencies since this parameter was the only one which differed in the two cavity experiments. In fact the variation of this parameter and L/D in the different experiments of figure 5 could explain the large scattering of data shown there. In addition, it is to be noted that the present mathematical model does predict the correct change in tone Strouhal number due to a change in L/θ. This can easily be seen in figure 16.

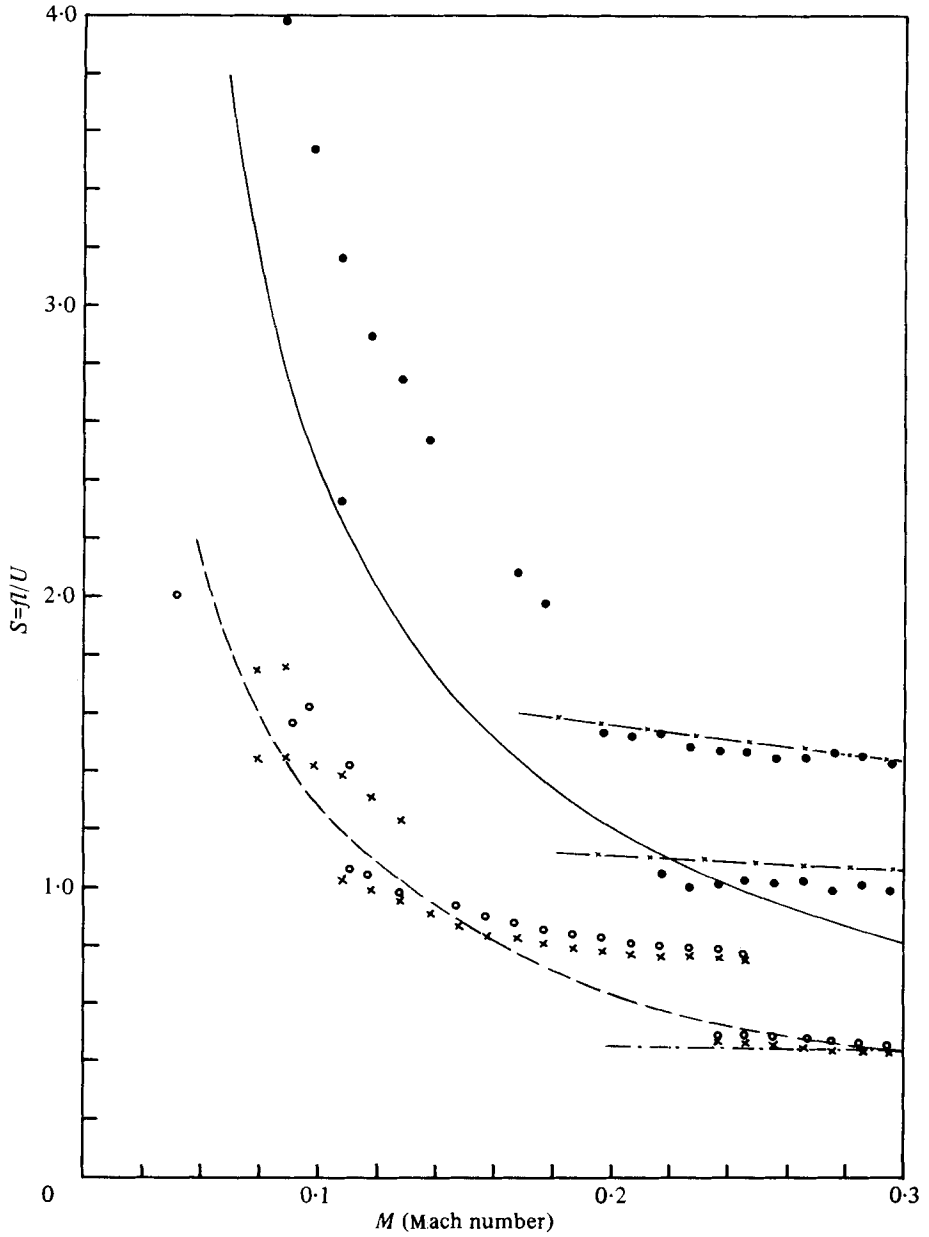

FIGURE 18. Discrete tone frequencies as a function of Mach number.

Data	L (cm)	D (cm)	L/D
○	4	5·08	0·787
×	2·5	3·175	0·787
●	7·5	3·175	2·36

Theoretical predictions: ——, equations (25); ×—×, equations (21) and (19), $L/2\theta = 70$; – – –, equations (24); —·—, equations (21) and (19), $L/2\theta = 50$.

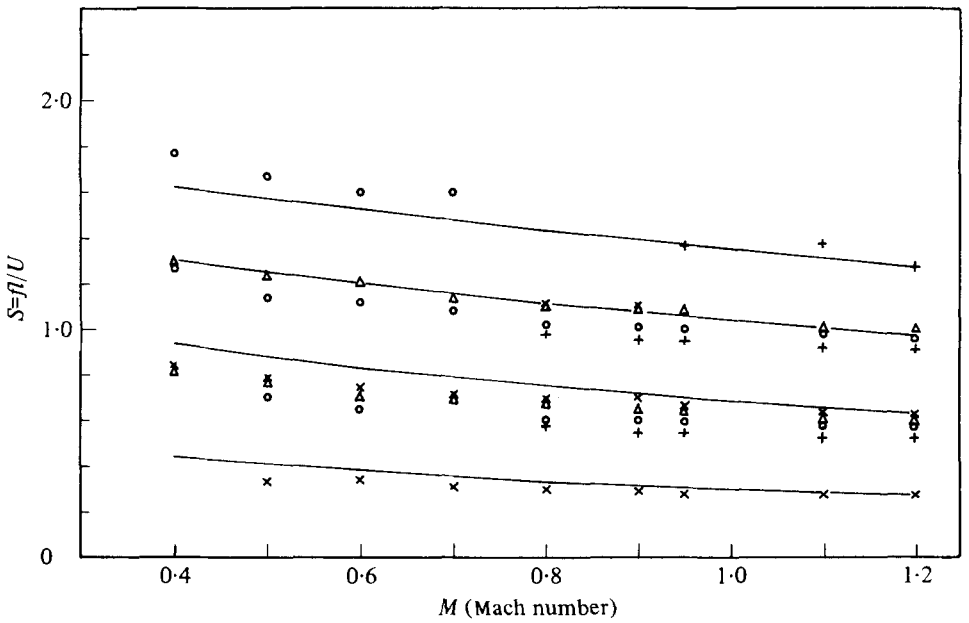

FIGURE 19. Discrete tone frequencies as a function of Mach number. Data from Rossiter (1964): ×, $L/D = 4$; △, $L/D = 6$; ○, $L/D = 8$; +, $L/D = 10$. ——, equations (21) and (19), $L/2\theta = 50$, $L/D = 4$.

Finally, the overall good agreement between the theoretically predicted and measured tone frequencies as demonstrated above must be regarded as lending concrete support to the contention that the present model does contain the essential physics of the feedback oscillation phenomenon.

Figure 18 shows the dependence of the Strouhal number of the discrete tones of deep cavities on flow Mach numbers at very low subsonic flow. For Mach numbers greater than 0·24, the Strouhal number–Mach number relationship is similar to that of shallow cavities, indicating that the tones are generated by the same feedback mechanism. As a matter of fact, the measured data agree very well with the predicted tone frequencies of the present model with $L/2\theta = 50$. The predicted Strouhal numbers are shown as a dot–dash curve in figure 18. For Mach numbers less than 0·15, the measured relationship between Strouhal number and Mach number clearly indicates that the tones are most probably generated by a different mechanism. The works of Plumblee *et al.* (1962) and East (1966) earlier suggested an alternative mechanism involving normal mode resonance. Here, however, we do not consider the source of energy which drives the resonance to be the broadband turbulence in the shear layer which spans the mouth of the cavity as Plumblee *et al.* originally proposed. Instead we believe that the energy is actually provided by shear layer instabilities. To test this idea one can compare the measured frequencies and the normal mode frequencies of the cavities. In a recent paper, Tam (1976) has computed several of the lower normal mode frequencies of two-dimensional rectangular cavities under the no flow condition. Since the flow Mach numbers under consideration are less than 0·15, the no flow model should be a reasonable approximation as far as resonance frequencies are concerned. Figure 20 shows the calculated frequency (ω is complex because of

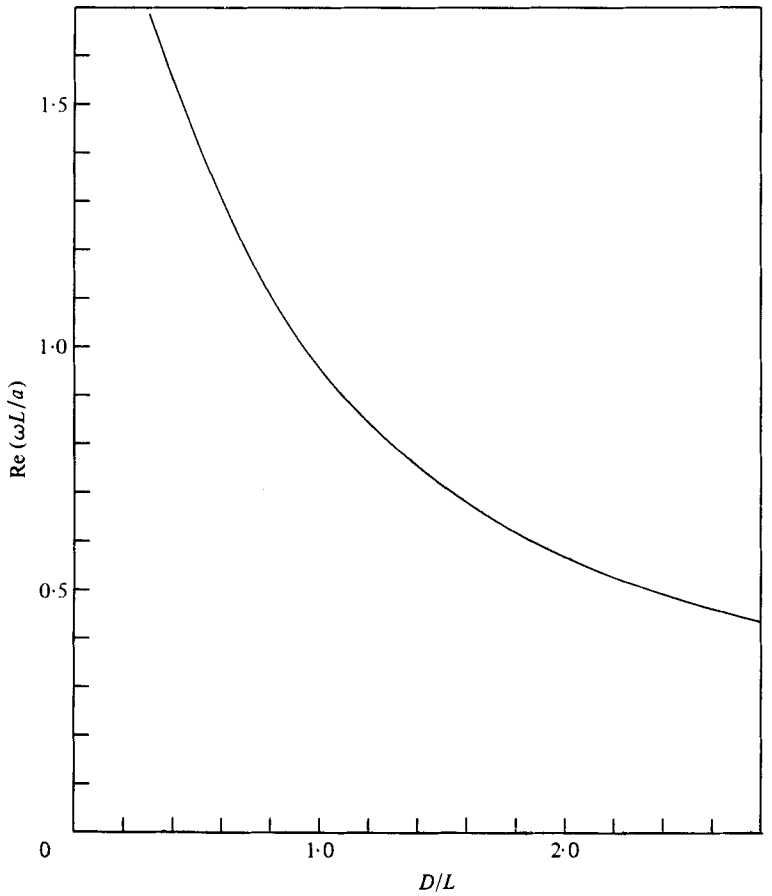

FIGURE 20. The real part of $\omega L/a$ *vs.* D/L of the (1, 1) mode or the depth mode of a two-dimensional rectangular cavity (Tam 1976).

radiation damping; only the real part of ω is shown in this figure) of the depth mode (lowest normal mode) as a function of the length to depth ratio of the cavity, i.e. L/D. For $L/D = 0{\cdot}787$, the depth mode frequency is $\omega L/a = 0{\cdot}8$. Upon rewriting this in terms of the Strouhal number and Mach number one finds that

$$\frac{fL}{\bar{U}_\infty} = \frac{0{\cdot}1273}{M}. \tag{24}$$

As shown in figure 18, (24) correlates the measured data very well, giving strong support to the normal mode resonance concept. For very low Mach numbers ($M < 0{\cdot}2$), the measured tone frequencies of the smaller shallow cavity ($L = 7{\cdot}5$ cm, $D = 31{\cdot}75$ cm, $L/D = 2{\cdot}36$) exhibit characteristics similar to those of deep cavities. To demonstrate this, let us compare the measured frequencies with the lowest-order normal mode frequency of such a cavity. From figure 20 the depth mode frequency for $L/D = 2{\cdot}36$ is $\omega L/a = 1{\cdot}517$, which gives

$$\frac{fL}{\bar{U}_\infty} = \frac{0{\cdot}2414}{M}. \tag{25}$$

Figure 18 shows a comparison between (25) and the measured data. Although quantitative agreement between the calculated and measured values is not as good as in the case of deep cavities, the shapes of the theoretical and measured curves exhibit a striking resemblance. It is believed that the quantitative difference is due primarily to the fact that the no flow model is less applicable in this case. With this qualification, one must conclude that the evidence is strongly in favour of normal mode resonance being the generation mechanism of these tones at very low subsonic Mach number.

6. Concluding remarks

In this paper, experimental measurements of cavity tone frequencies at low subsonic Mach numbers ($M < 0{\cdot}4$) are presented. A mathematical model of the cavity pressure oscillation and acoustic feedback is also developed. This model accounts for the finite shear layer thickness effects and acoustic reflexions from the bottom and upstream end walls of the cavity which have not been considered by existing models. These features are shown to be important by comparison of predicted and measured tone frequencies. Overall good agreement is found between predicted discrete tone frequencies of the proposed model and the data of Rossiter ($0{\cdot}4 \leqslant M \leqslant 1{\cdot}2$) and also our own data for flow Mach number greater than 0·2. For very low subsonic Mach number, $M < 0{\cdot}2$, evidence is found which suggests that the tones are generated by the normal mode resonance mechanism. The transition between the feedback mechanism and normal mode resonance mechanism-generated tones seems to be rather gradual (as evidenced by examining the measured data carefully). This indicates that a unified model of the phenomenon of flow-induced cavity tones is possible. Actually the present proposed model could serve as a basis for such a unified theory. In the development of the present model, the reflexions of acoustic waves at the open end of the cavity were neglected. This necessarily, therefore, rules out the possibility of cavity normal mode resonance. From a practical standpoint of aircraft wheel well cavity noise, tones generated by the normal mode resonance mechanism are of little significance. In order for a commercial aircraft to stay above the ground it must maintain a minimum speed of generally greater than or equal to $M = 0{\cdot}2$. Thus the switch-over from feedback mechanism to the normal mode resonance mechanism would occur only after the aircraft has landed. Because of this, this phenomenon will not be pursued in this work. However, it is anticipated that an extension of the present model to include the reflexions at the open end of the cavity and secondary reflexions from cavity walls and possible standing acoustic waves inside the cavity due to these reflexions would give a complete prediction of cavity tone frequencies for the full range of subsonic and supersonic flow Mach numbers.

Most of this work was done while one of the authors (CKWT) was visiting the N.A.S.A. Langley Research Center on a leave of absence from the Florida State University. The completion of this work was supported by N.A.S.A. Grant NSG 1329.

REFERENCES

Bilanin, A. J. & Covert, E. E. 1973 Estimation of possible excitation frequencies for shallow rectangular cavities. *A.I.A.A.J.* **11**, 347-351.

Block, P. J. W. 1976 Noise response of cavities of varying dimensions at subsonic speeds. *N.A.S.A. Tech. Note* D-8351.

BRIGGS, R. J. 1964 *Electron Stream Interactions with Plasmas*. M.I.T. Press.

CHAMPAGNE, F. H., PAO, Y. H. & WYGNANSKI, I. J. 1976 On the two-dimensional mixing region. *J. Fluid Mech.* **74**, 209–250.

CHAN, Y. Y. 1974*a*, *b* Spatial waves in turbulent jets. *Phys. Fluids* **17**, 46–53, 1667–1670.

CHAN, Y. Y. 1976 Spatial waves of higher modes in an axisymmetric turbulent jet. *Phys. Fluids* **19**, 2042–2043.

CHAN, Y. Y. 1977 Wavelike eddies in a turbulent jet. *A.I.A.A. J.* **15**, 992–1001.

COVERT, E. E. 1970 An approximate calculation of the onset velocity of cavity oscillations. *A.I.A.A. J.* **8**, 2189–2194.

DUNHAM, W. H. 1962 Flow induced cavity resonance in viscous compressible and incompressible fluids. *4th Symp. Naval Hydrody. Propulsion Hydroelasticity*, paper ACR-92, p. 1057–1081.

EAST, L. F. 1966 Aerodynamically induced resonance in rectangular cavities. *J. Sound Vib.* **3**, 277–287.

GIBSON, J. S. 1974 Non-engine aerodynamic noise investigation of a large aircraft. *N.A.S.A. Contractor Rep.* no. 2378.

GOTTLIEB, P. 1960 Sound source near a velocity discontinuity. *J. Acoust. Soc. Am.* **32**, 1117–1122.

HEALY, G. J. 1974 Measurements and analysis of aircraft far-field aerodynamic noise. *N.A.S.A. Contractor Rep.* no. 2377.

HELLER, H. H. & BLISS, D. B. 1975 The physical mechanism of flow induced pressure fluctuations in cavities and concepts for their suppression. *A.I.A.A. Paper* no. 75–491.

HELLER, H. H., HOLMES, D. G. & COVERT, E. E. 1971 Flow-induced pressure oscillations in shallow cavities. *J. Sound Vib.* **18**, 545–553.

KRISHNAMURTY, K. 1955 Acoustic radiation from two-dimensional rectangular cutouts in aerodynamic surfaces. *N.A.C.A. Tech. Note* no. 3487.

LIEPMAN, H. W. & LAUFER, J. 1974 Investigation of free turbulent mixing. *NA.C.A. Tech. Note* no. 1257.

LIN, C. C. 1955 *Theory of Hydrodynamic Stability*. Cambridge University Press.

MAULL, D. J. & EAST, L. F. 1963 Three-dimensional flow in cavities. *J. Fluid Mech.* **16**, 620–632.

MICHALKE, A. 1965 On spatially growing disturbances in an inviscid shear layer. *J. Fluid Mech.* **23**, 521–544.

MILES, J. W. 1958 On the disturbed motion of a plane vortex sheet. *J. Fluid Mech.* **4**, 538–552.

MOORE, C. J. 1977 The role of shear-layer instability waves in jet exhaust noise. *J. Fluid Mech.* **80**, 321–367.

PATEL, R. P. 1973 An experimental study of a plane mixing layer. *A.I.A.A. J.* **11**, 67–71.

PLUMBLEE, H. E., GIBSON, J. S. & LASSITER, L. W. 1962 A theoretical and experimental investigation of the acoustic response of cavities in an aerodynamic flow. *U.S. Air Force Rep.* WADD-TR-61-75.

ROSHKO, A. 1955 Some measurements of flow in a rectangular cutout. *N.A.C.A. Tech. Note* no. 3488.

ROSSITER, J. E. 1964 Wind tunnel experiments of the flow over rectangular cavities at subsonic and transonic speeds. *Aero. Res. Counc. R. & M.* no. 3438.

SCHLICHTING, H. 1960 *Boundary Layer Theory*. McGraw-Hill.

SPEE, B. M. 1966 Wind tunnel experiments on unsteady cavity flow at high subsonic speeds. *AGARD Current Paper* no. 4, pp. 941–974.

TAM, C. K. W. 1971 Directional acoustic radiation from a supersonic jet generated by shear layer instability. *J. Fluid Mech.* **46**, 757–768.

TAM, C. K. W. 1976 The acoustic modes of a two-dimensional rectangular cavity. *J. Sound Vib.* **49**, 353–364.

WYGNANSKI, I. J. & FIEDLER, H. E. 1970 The two-dimensional mixing region. *J. Fluid Mech.* **41**, 327–361.